ISSN: 0067-2904

The Effect of Silver Oxide on the Structural and Optical Properties of ZnO: AgO Thin Films

Hawraa H. Abbas*, Bushra A. Hasan
Department of Physics, College of Science, University of Baghdad, Baghdad, Iraq

Received: 19/4/2021 Accepted: 19/6/2021 Published: 30/4/2022

Abstracts
Compounds from ZnO doped with AgO in different ratio (0,3,5,7, and 9)wt.% were prepared.Thin films from the prepared compounds were deposited on a glass substrate using the pulsed laser deposition method. The XRD pattern confirmed the presence of a single-phase hexagonal wurtzite ZnO structure, without the presence of a secondary phase. AFM measurements showed an increase in both average grain size and average surface roughness with increasing concentration content of (AgO).The crystallite size of ZnO of the main peak corresponding to the preferred plane of crystal growth named (100) increases from 17.8 to 22.5nm by increasing of AgO doping ratio from 0 to 9%. The absorbance and transmittance in the wavelength range (350-1100 nm) were used to determine the optical properties. The results showed that the optical energy gap for direct allowed transition (r =0.5)are (3.21, 3.2,3.15, 3.15, 2.95) Ev, respectively. The optical constants were also measured as a function of wavelength. This optical measurements showed the prepared thin film have many applications for solar cell fabrication and sensing devices.

Keywords: ZnO: AgO thin films, Energy gap, X-ray diffraction, pulsed laser deposition PLD

تأثير إضافة أكسيد الفضة في الخصائص التركيبية والبصرية للأغشية الرقيقة ZnO: AgO

حوراء هادي عباس* , بشرى عباس حسن
قسم الفيزياء ، كلية العلوم ، جامعة بغداد ، بغداد ، العراق

الخلاصه

تم تحضير مركبات من ZnO المطعم باوكسيد الفضة بنسب مختلفة .(0,3,5,7and 9)wt%,تم ترسيب أغشية رقيقة من المركبات المحضرة على قواعد زجاجية باستخدام طريقة الترسيب بالليزر النبضي. أكد طيف حيود الاشعة السينية وجود هيكل Wurtzite ZnO السداسي أحادي الطور ، دون وجود طور ثانوي. لقد ازداد الحجم البلوري لـ ZnO للقمة الرئيسية المقابلة للمستوى المفضل لنمو البلورات عند (100) من 17.8 إلى 22.5 نانومتر مع زيادة نسبة التشويب باوكسيد الفضة من 0 إلى 9٪. أظهرت قياسات AFM زيادة في كل من متوسط حجم الحبوب ومتوسط خشونة السطح مع زيادة محتوى تركيز (AgO).تم استخدام الامتصاصية والنفاذية في مدى الطول الموجي (350–1100 نانومتر) لتحديد الخواص البصرية. اظهرت النتائج أن فجوة الطاقة البصرية للانتقال المباشر المسموح (r = 0.5) هي (3.21 ، 3.2 ، 3.15 ، 3.15

*Email: Hawraa.Abbas1204@sc.uobaghdad.edu.iq

، 2.95) الكترون–فولت على التوالي. تم قياس الثوابت البصرية أيضًا كدالة للطول الموجي. لقد اظهرت القياسات البصرية ان الاغشية المحضرة لها تطبيقات كثيرة في تصنيع الخلايا الشمسية والمتحسسات.

Introduction

Scientists and industries all over the world are interested in zinc oxide (ZnO) nanoparticles, which are a potential photoluminescence material with strong oxidation capability, non-toxicity, chemical stability, and a phenomenally low cost. It was found that luminescence effects of ZnO nano-particles at primary blue and red changes on their Near Band Edge (NBE) emissions would be affected by doping and visible emission improvements which were made to be long-lasting.[1]

Several experimental and theoretical aspects studies in different morphologies like nanoparticles, nanowires, and thin films with nanostructure were carried out due to their special optoelectronic characteristics, electric transducer transducers, instruments optoelectronic, space sensors, sensors, windows of the solar cell, and other applications. Pure ZnO nanoparticles do not meet the practical needs as a photocatalytic material, as activation of ZnO catalyst necessitates high-energy UV light, leading to low efficiency in the visible and near infrared regions. The rapid recombination of the photogenerated e^- /h• pairs is another limiting factor that impedes the photocatalytic activity of ZnO nanoparticle[2]. ZnO is a compound semiconductor with a large range bandgap at room temperature (3.36 eV) and a high energy for the excitonic binding process (60eV) [3]. Morphology, development technique, synthesis, conditions of synthesis, and defects of these nanostructures influence ZnO nanoparticles luminescence properties. On semiconductor nanostructures, Ag-doped ZnO particles photocatalyst effect has a distinct effect. Additionally, Ag-doped ZnO particles are bioconsistent, biosafe, and of intracellular phototoxic content [4]. Metal ions doped in Ag-doped ZnO particles are utilized for a variety of applications at room temperature, including n-type doped nanolasers and p-type doping as semiconductor ferromagnetic material. Transition metals with lower levels of Fermi energy are highly absorbed optically, stimulating the mechanism of interfacial electron transfer[5]. The AgO :ZnO thin films can be prepared by a variety of methods [6], such as chemical vapor deposition(CVD)[7], magnetron sputtering[8], pulsed laser deposition(PLD)[9], spray pyrolysis[10] , molecular beam epitaxy (MBE)[11], and sol–gel technique[12]. In this work, the preparation of undoped and AgO-doped ZnO composites deposited on a glass substrate by pulsed laser deposition technique was reported. The structural and optical properties of these films were studied.

Experimental part:

The starting materials in this work: ZnO and AgO (of high purity, three nines after digit)were provided by Aldrich. The compounds with different doping ratios were weighted according to the atomic weight using an electronic balance with four digits after the point (10^{-4} gm)company. The mixtures of the two oxides were sintered by putting the mixture in quartz ampoule with length ~ 25 cm and internal diameter ~ 8 mm, evacuated to ~10^{-3} Torr, sealed and put in an oven and heated to 1273K for 5 hours,after which they were left to cool at room temperature. The obtained materials were grounded to obtain a homogeneous powder and pressed into pellets, with a diameter of 1 cm and 0.5 cm thick, with hydraulic piston(type (SPECIAL), under a pressure of 7 tons for 10 min. AgO doped zinc oxide thin films with various doping ratios (0, 0.03, 0.05,0.07, and 0.09) were deposited using the pulsed laser deposition technique. The deposition was done under vacuum of $2x10^{-2}$ Torr with Nd: YAG laser beam (of energy, pulsed, and frequency of 500 mJ,500, and 6Hz, respectively)which was focused through a window to be incident on the target. The ablated atoms were incident on the glass substrates and get gathered to create the thin films.

The optical interferometer method was used to determine the film thickness (t) using the following equation[13]:

$$t = \frac{\lambda}{2}\frac{\Delta x}{x} \quad \text{----------(1)}$$

Where Δx, x, and λ are the shift of the interference fringes, the distance between the interference fringes, and the wavelength of He: Ne (632.8nm), respectively. The XRD measurements were conducted at (the Iranian Republic laboratories) using a diffractometer (type XRD / 6000 Shimadzu) with Cu-Kα (λ= 1.5404 Å) radiation, operated at 30 kV, 20 mA**.** The average crystal size (D) was calculated using Scherrer formula [14] :

$$D = \frac{0.9\lambda}{\beta\cos\theta} \quad \text{----------(2)}$$

where β and θ are the full widths at half maximum and the glancing angle, respectively. The dislocations density and the strain δ were determined by applying the following relations:

$$\delta = \frac{1}{D^2} \quad \text{----------(3)}$$

and

$$\Delta = \frac{D\cos\frac{\delta}{2}}{4} \quad \text{---------(4)}$$

respectively.

The lattice constant a for (100) plane was determined by the following relation[15] ,

$$a=\lambda/\sqrt{3}\sin\theta \quad \text{----------(5)}$$

While, the lattice constant c for the (002) plane was determined by the relation,[15]

$$c= \lambda/ \sin\theta - \quad \text{----------(6)}$$

At normal incidence , a double-track spectrometer (A double -beam UV/Vis spectrophotometer (Metertech) SP8001) was used to obtain the optical transmission and absorption spectra for the pulsed deposited film samples from the deposited thin films with an absorbent computer data collection and wavelength transmission range between 200 and 1100 nm. The absorption coefficient of the thin films was determined by applying the given relation [16]:

$$\alpha =2.303\ A/t \quad \text{----------(7)}$$

where t and A are the thickness and absorption of the thin film sample,respectively.

The optical band gap for direct allowed transition was determined by applying Tauc relation [17]:

$$(\alpha h\nu)^{1/r} = B\ (h\nu - E_{gopt}) \quad \text{----------(8)}$$

where hν, E_{gopt}, and B are the photon energy, the optical band gap, and band tailing parameter, respectively, Real and imaginary dielectric constants were computed by applying the following relations[16]:

$$\varepsilon_r = n2-k2 \quad \text{----------(9)}$$

$$\varepsilon_i = 2nk \quad \text{----------(10)}$$

using the concepts of refraction index (n) and extinction coefficient (k), the optical properties of semiconductors can also be determined using the following relations. [18]:

$$n = [4R/(R-1)^2 - K^2]^{1/2} - (R+1)/(R-1) \quad \text{----------(11)}$$

$$K=\alpha\lambda/4\pi- \quad \text{----------(12)}$$

Where R and λ are the reflectance and the wavelength of incident photon, respectively

Results and Discussion:

X-ray diffraction analysis is known as a good criterion to know the phase of the prepared samples. Figure 1 shows the X-ray diffraction patterns of ZnO prepared with different AgO doping ratios which were compatible with the standard diffraction peaks of wurtzite structure ZnO (JCPDS 96-230-0114). The observed diffraction peaks matched the (100) (002), and (101) reflections of the ZnO wurtzite structure[19][20]. No peaks corresponding to the AgO phase were found which demonstrates that single phase of AZO was formed at low doping ratio i.e up 7%. Tiny peaks related to AgO were observed at a 9% doping ratio. The observed diffraction coincides with the (20-2) and (31-1)of AgO monoclinic structure standard cards (96-900-8963). The X-ray diffraction data also showed that the reflection peaks intensity of the doped films depended strongly on the doping ratio. ZnO thin films and residual doped thin films exhibited preferred (100) orientation. As the doping ratio was increased the (100) and (101) reflections of the film increased. This phenomenon can be attributed to the diffusion of atoms absorbed on the substrate and are accelerated to the migration of atoms to more energy favorable positions, resulting in the enhancement of the polycrystallinity of film and initiating grain growth which is indicated by the increment of (100), (101) reflections. Indeed the crystal size had grown from 17.8 to 22.4 nm by increasing the doping ratio from 0 to 0.09%. It can be noticed that the diffraction peaks positions of doped thin films with 3%AgO as compared to that of undoped ZnO had shifted toward larger angle direction, indicating a decrease of the unit cell lattice parameters resulting from the incorporation of Ag (0.57Å), with smaller atomic size than Zn (0.60Å)[21] .The peak clearly shows that the incorporation of Ag dopant with low ratio leads to a clear reduction in crystallite size. In contrast , the diffraction peaks of the 0.05, and 0.07 doping ratio samples shifted to smaller diffraction angles indicating an increase of the unit cell lattice parameters [17]. In the literature review, Ag can integrate conformity into the ZnO, which replaces Zn^{2+} or as an intermediated space atom[22], according to the findings of others. The Ag dopant as a replacement for Zn^{2+} helps to bring the XRD closer to the maximum[23].

By increasing AgO concentration, peaks positions were shifted , as shown in Table 1.This suggests that adding AgO to zinc oxide at low doping ratio (3%) leads to an intermediated space atom and a reduction of crysttalite size, while doping of ratios (5, 7, and 9 %) suggests the partial substitution of Ag+ ions at the ZnO lattice and increase in the crysttalite size. This issue is presumably related to the ionic size difference between the Ag+ (0.126 nm) and Zn^{2+} (0.074 nm) ions[24]. The dislocation density of the prepared thin films exhibits to change in opposite to that of crystal size. The dislocation density and the strain was reduced from 3.15 x1015 to 1.98 x1015 (line / m2) and from 0.0019 to 0.0015 by the continuous addition of silver oxide to the host oxide (ZnO).

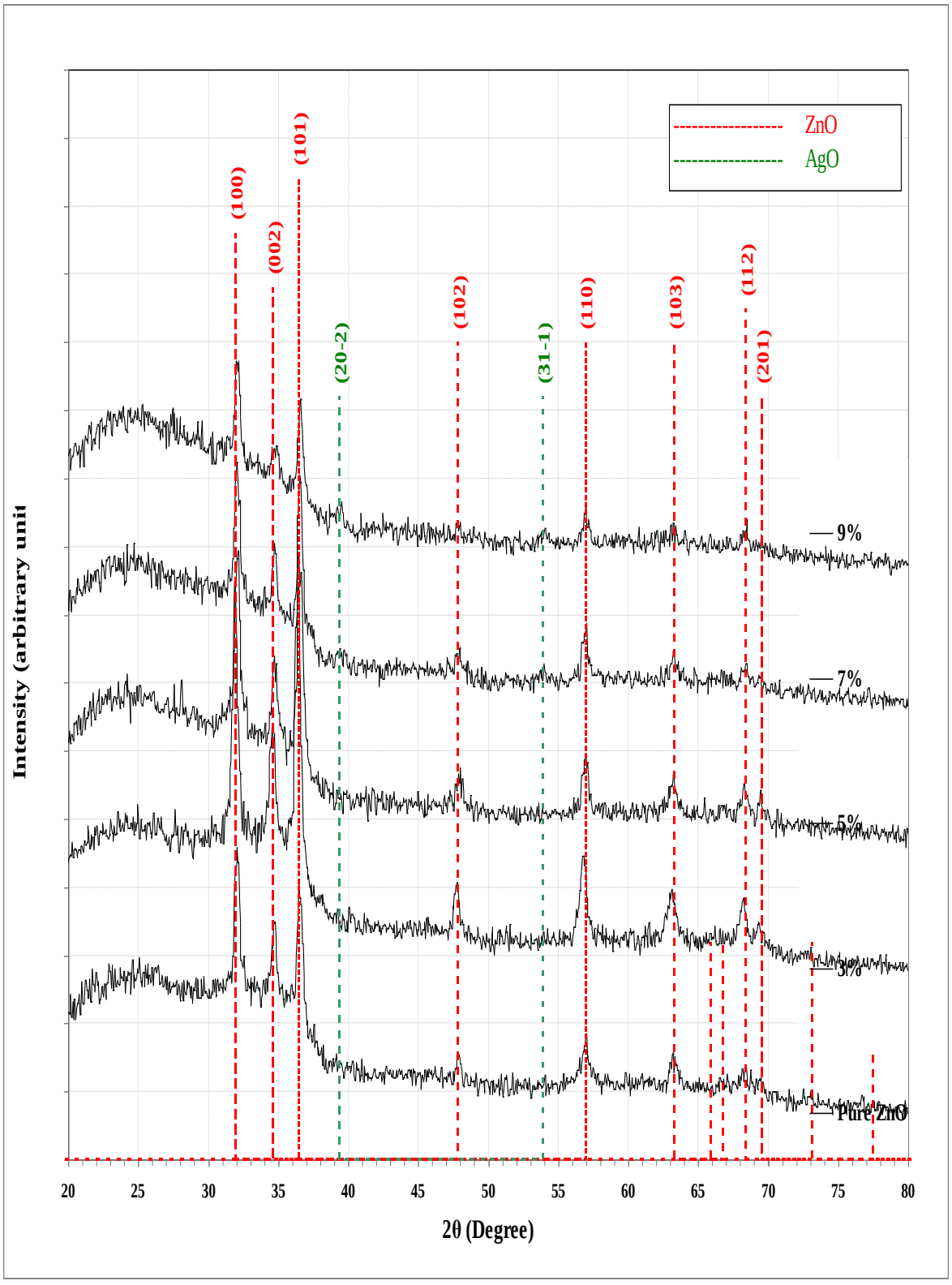

Figure 1-(XRD) patterns of ZnO:AgO thin films prepared by PLD technique

Table 1- Analysis of (XRD) for ZnO:AgO thin films prepared by PLD technique

AgO %	2θ (Deg.)	FWHM (Deg.)	d_{hkl} Exp.(Å)	C.S (nm)	hkl	d_{hkl} Std.(Å)	Phase	Card No.	$\delta \times 10^{15}$ (line/m)	strain
0	32.0357	0.4643	2.7916	17.8	(100)	2.7989	Hex. ZnO	96-230-0114	3.15	0.0019
	34.6786	0.5000	2.5846	16.7	(002)	2.5867	Hex. ZnO	96-230-0114	3.61	0.0021
	36.4286	0.5000	2.4644	16.7	(101)	2.4617	Hex. ZnO	96-230-0114	3.57	0.0021
	47.8214	0.4643	1.9005	18.7	(102)	1.8994	Hex. ZnO	96-230-0114	2.85	0.0019
	56.9286	0.5714	1.6162	15.8	(110)	1.6156	Hex. ZnO	96-230-0114	4.00	0.0022
	63.1429	0.7143	1.4713	13.1	(103)	1.4680	Hex. ZnO	96-230-0114	5.86	0.0027
	68.3214	0.8214	1.3718	11.7	(112)	1.3703	Hex. ZnO	96-230-0114	7.32	0.0030
	69.4286	0.6071	1.3526	15.9	(201)	1.3507	Hex. ZnO	96-230-0114	3.94	0.0022
3%	31.8856	0.5718	2.8044	14.5	(100)	2.7989	Hex. ZnO	96-230-0114	4.79	0.0024
	34.5405	0.4902	2.5947	17.0	(002)	2.5867	Hex. ZnO	96-230-0114	3.47	0.0020
	36.4602	0.5310	2.4623	15.8	(101)	2.4617	Hex. ZnO	96-230-0114	4.03	0.0022
	47.7332	0.4493	1.9038	19.3	(102)	1.8994	Hex. ZnO	96-230-0114	2.67	0.0018
	56.7597	0.5718	1.6206	15.8	(110)	1.6156	Hex. ZnO	96-230-0114	4.01	0.0022
	63.0088	0.8168	1.4741	11.4	(103)	1.4680	Hex. ZnO	96-230-0114	7.68	0.0030
	68.2369	0.6127	1.3733	15.7	(112)	1.3703	Hex. ZnO	96-230-0114	4.07	0.0022
	69.3397	0.5310	1.3541	18.2	(201)	1.3507	Hex. ZnO	96-230-0114	3.02	0.0019
5%	32.0707	0.4493	2.7886	18.4	(100)	2.7989	Hex. ZnO	96-230-0114	2.95	0.0019
	34.6630	0.4492	2.5858	18.5	(002)	2.5867	Hex. ZnO	96-230-0114	2.91	0.0019
	36.6036	0.5309	2.4530	15.8	(101)	2.4617	Hex. ZnO	96-230-0114	4.02	0.0022
	47.9782	0.6535	1.8947	13.3	(102)	1.8994	Hex. ZnO	96-230-0114	5.64	0.0026
	56.9639	0.5718	1.6153	15.8	(110)	1.6156	Hex. ZnO	96-230-0114	4.00	0.0022
	63.2131	0.5718	1.4698	16.3	(103)	1.4680	Hex. ZnO	96-230-0114	3.76	0.0021
	68.2369	0.6535	1.3733	14.7	(112)	1.3703	Hex. ZnO	96-230-0114	4.64	0.0024
	69.4622	0.5718	1.3521	16.9	(201)	1.3507	Hex. ZnO	96-230-0114	3.50	0.0021
	32.0690	0.4493	2.7888	18.4	(100)	2.7989	Hex. ZnO	96-230-0114	2.95	0.0019
	34.7039	0.4084	2.5828	20.4	(002)	2.5867	Hex. ZnO	96-230-0114	2.41	0.0017
	36.5010	0.3676	2.4597	22.8	(101)	2.4617	Hex. ZnO	96-230-0114	1.93	0.0015
	39.4418	0.8168	2.2828	10.3	(20-2)	2.2812	AgO	96-900-8963	9.36	0.0034
	47.8557	0.6127	1.8992	14.2	(102)	1.8994	Hex. ZnO	96-230-0114	4.97	0.0024

7%	53.9006	0.8169	1.6996	10.9	(31-1)	1.6979	AgO	96-900-8963	8.40	0.0032
	56.9231	0.4084	1.6163	22.1	(110)	1.6156	Hex. ZnO	96-230-0114	2.04	0.0016
	63.2131	0.4493	1.4698	20.8	(103)	1.4680	Hex. ZnO	96-230-0114	2.32	0.0017
	68.3186	0.5718	1.3719	16.8	(112)	1.3703	Hex. ZnO	96-230-0114	3.55	0.0021
	69.4622	0.5718	1.3521	16.9	(201)	1.3507	Hex. ZnO	96-230-0114	3.50	0.0021
9%	32.1307	0.3676	2.7835	22.5	(100)	2.7989	Hex. ZnO	96-230-0114	1.98	0.0015
	34.6630	0.5718	2.5858	14.6	(002)	2.5867	Hex. ZnO	96-230-0114	4.72	0.0024
	36.5419	0.4085	2.4570	20.5	(101)	2.4617	Hex. ZnO	96-230-0114	2.38	0.0017
	39.4418	0.6535	2.2828	12.9	(20-2)	2.2812	AgO	96-900-8963	5.99	0.0027
	47.9374	0.5718	1.8962	15.2	(102)	1.8994	Hex. ZnO	96-230-0114	4.32	0.0023
	53.9823	0.8577	1.6972	10.4	(31-1)	1.6979	AgO	96-900-8963	9.25	0.0033
	56.9231	0.5718	1.6163	15.8	(110)	1.6156	Hex. ZnO	96-230-0114	4.00	0.0022
	63.2131	0.6535	1.4698	14.3	(103)	1.4680	Hex. ZnO	96-230-0114	4.90	0.0024
	68.4003	0.6944	1.3704	13.8	(112)	1.3703	Hex. ZnO	96-230-0114	5.22	0.0025
	69.5031	0.8169	1.3514	11.8	(201)	1.3507	Hex. ZnO	96-230-0114	7.13	0.0029

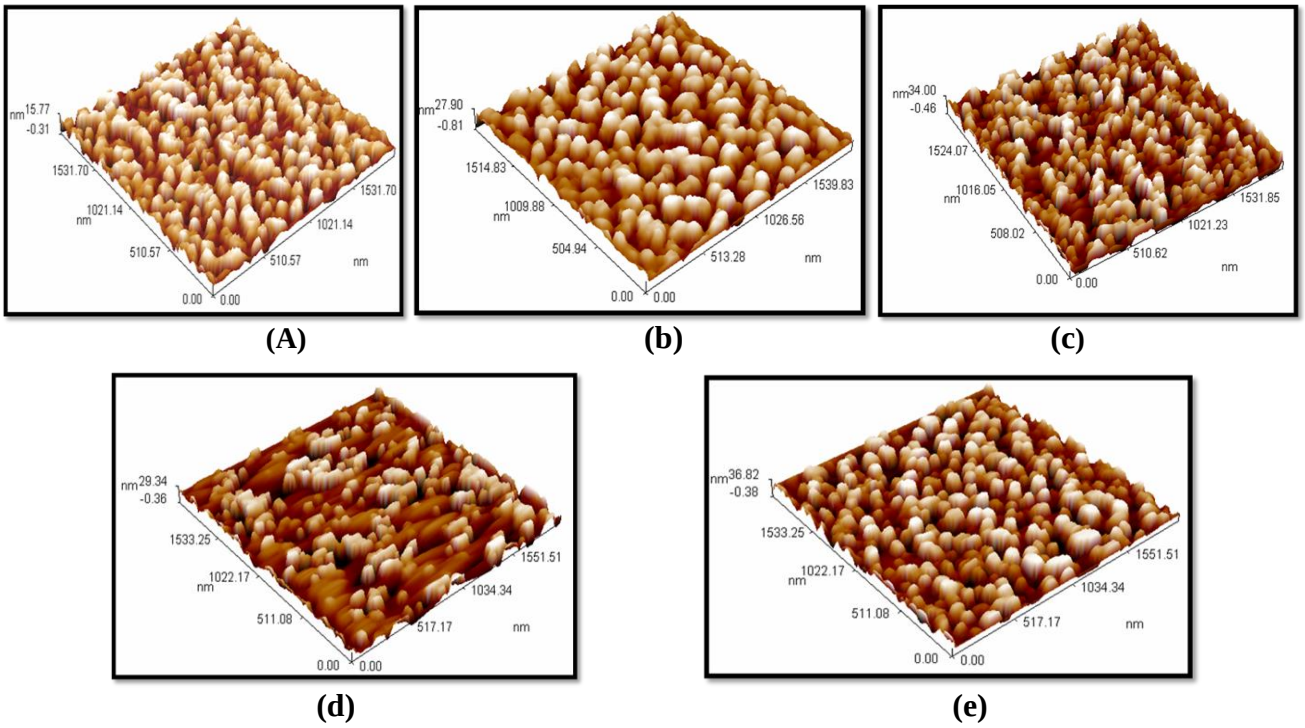

Figure 2- AFM images of: (a) puerZnO (b) ZnO : 3 wt%AgO (c) ZnO: 5 wt%AgO (d) ZnO:7wt%AgO (e) ZnO:9wt%AgO

Table 2-Average of the surface roughness and the granular size for the prepared films (ZnO:AgO)

Wt%	*Average Diameter (nm)*	*Roughness (nm)*	*RMS* (nm)	*Peak-Peak (nm)*
3 wt%	**62.56**	**5.56**	**6.67**	**28.7**
5wt%	**52.33**	**7.91**	**9.22**	**34.5**
7wt%	**60.33**	**6.16**	**7.45**	**29.6**
9wt%	**86.45**	**9.25**	**10.7**	**37.2**

The atomic force microscope 3D images, shown in Figure 2, shows pure zinc oxide films doped with silver oxide of different ratios (3,5,7,9) wt%. It was noticed that the increase in the ratio of silver oxide increased the surface roughness as well as the (RMS).They increased to values of 9.25 nm and 10.7 nm,respectively at a doping ratio of 9wt%. These values and those of the other AgO doping ratios are shown in Table 2. This result is in agreement with that of Karyaoui et al. [25].

Figure 3 shows the transmission spectrum of ZnO: AgO thin films with different doping ratios(0, 3, 5, 7 and 9 wt.%). It is clearly shown that the addition of AgO to ZnO led to a redshift, i.e. the absorption edge shifted towards longer wavelengths which is accompanied by a substantial reduction of the transparency of the thin films.

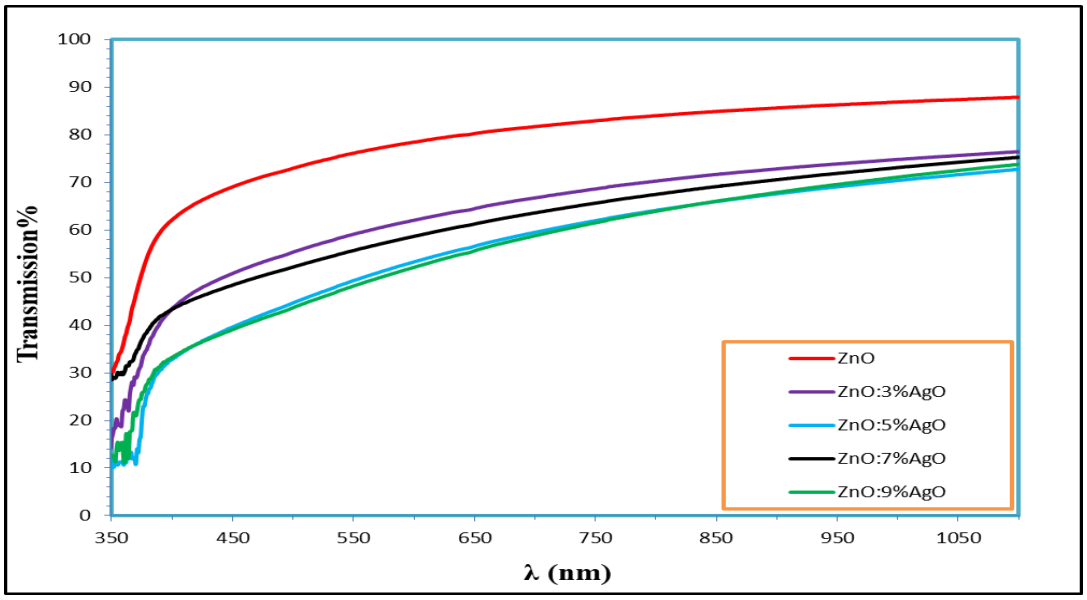

Figure 3- Transmittance spectrum as a function of wavelength for ZnO:AgO thin films at different doping ratios prepared by PLD technique..

Optical transmission is a well-known complicated function that is strongly influenced by the absorption coefficient (α).

Figure 4 shows the relation between $(\alpha hv)^2$ and (hv). By extrapolating the best fit linear part of the curve, the optical band gap Eg^{opt} can be estimated. Our results showed that the optical band gap was reduced by increasing the silver oxide concentration up to 7wt% and then the blue shift takes place which can be due to transitions from different defect levels of metal oxides to the O 2p band[26]. Sutanto et al.[27] pointed out that AgO-doped ZnO edge moved toward the visible light wavelengths. This optical observation showed a very good thin film for photocatalyst and other applications. While Ali et al. [28]refered that the energy band gap of the pure and doped ZnO thin films increased with the AgO doping. This increase of the energy band gap is known as the Moss-Burstein shift[29] . Because of this, at high doping levels of zinc oxide films, the donor electrons occupy the states at the lower edge of the

conduction band. Therefore, the optical band gap of AgO doped ZnO is greater than that of pure zinc oxide films.

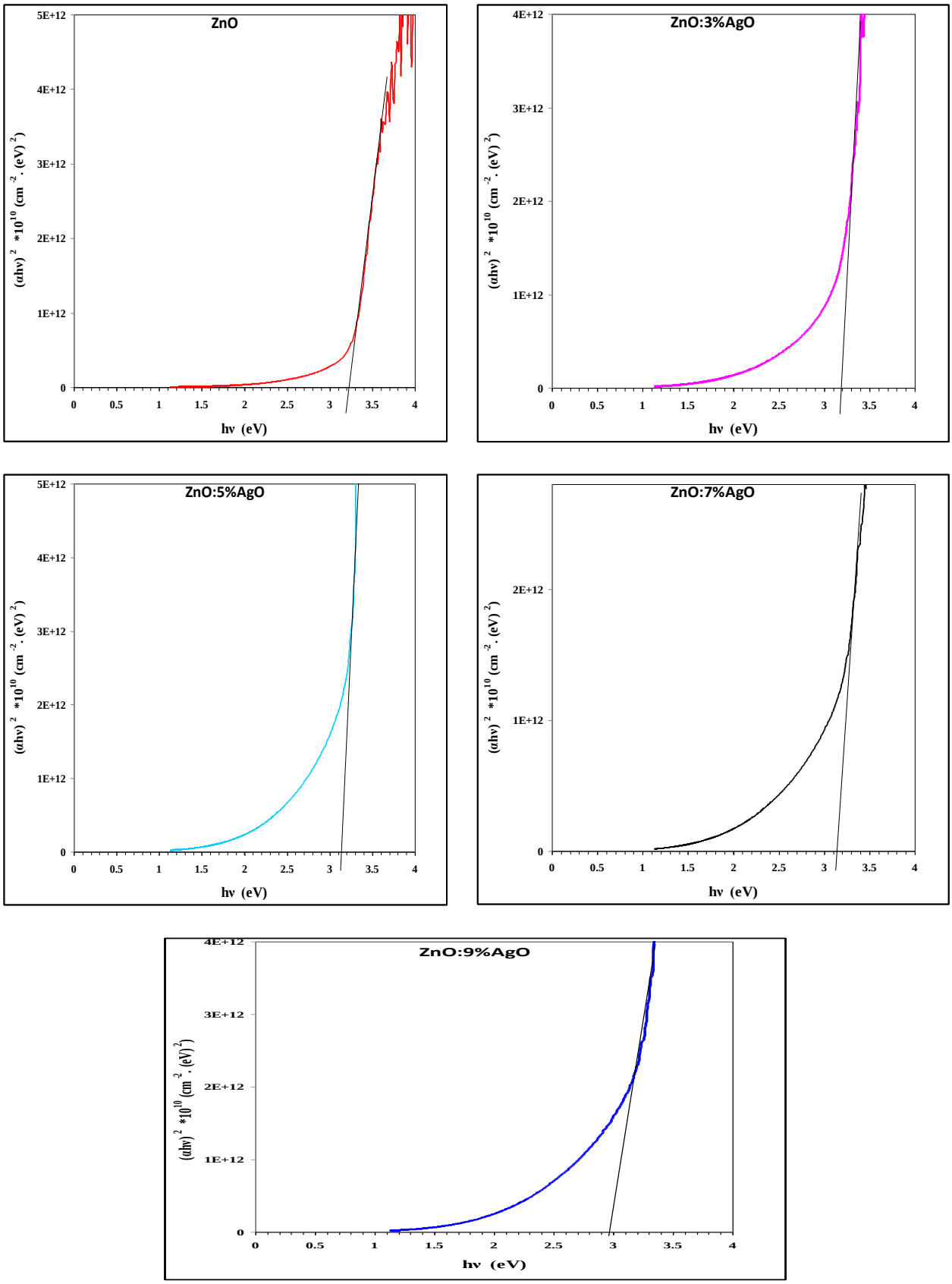

Figure 4-$(\alpha h\upsilon)^2$ versus $(h\upsilon)$ for ZnO:AgO thin films prepared by PLD technique.

The structure of the ZAO System may explain this variation in the optical bandgap. The relation between the refractive index n and the extinction coefficient k and wavelength are shown in Figures 5 and 6. It is observed that n and k grow up by the addition of AgO up to 5% then fall to lower values but then return to grow up again. The addition of AgO makes the prepared AZO more compact (increasing the packing density), which decreases the propagation velocity of light through the sample, thus increasing the n values, since n represents the ratio of light velocity through the vacuum to velocity through any medium.While, the behavior explanation of k is due to the growth of absorption coefficient, which represents the ratio of light velocity through the vacuum to velocity through any medium. The reduction of n and k with the further increase of AgO concentration i.e. to (7%) can be explained as follows :the addition of AgO makes ZnO less dense (or more transparent) which consequently decreases the packing density and in turn increases the light velocity through the sample and so reducing the refractive index.The reduction of k is attributed to the reduction of absorption coefficient .

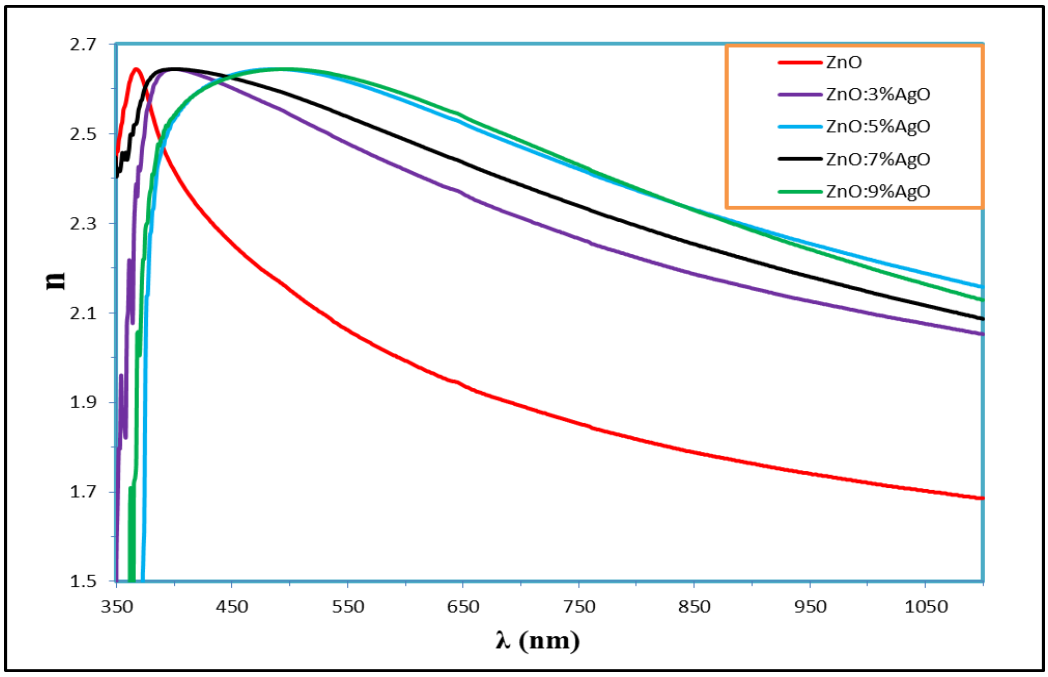

Figure 5- The plot diagram of n versus wavelength for ZnO:AgO thin films prepared by PLD technique.

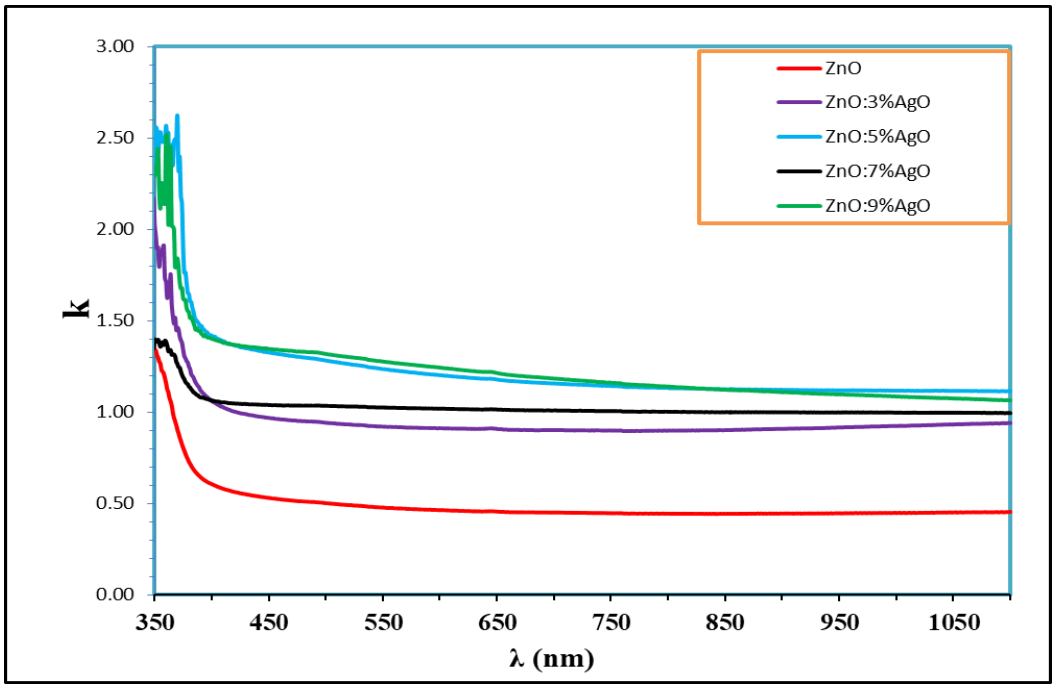

Figure 6: The plot diagram of K versus wavelength for ZnO:AgO thin films prepared by PLD technique.

Figures 7 and 8 show the relation between ε_r and ε_i and λ. It is remarked that ε_r and ε_i have the same trend of n and k, respectively thus similar explanation can be given.

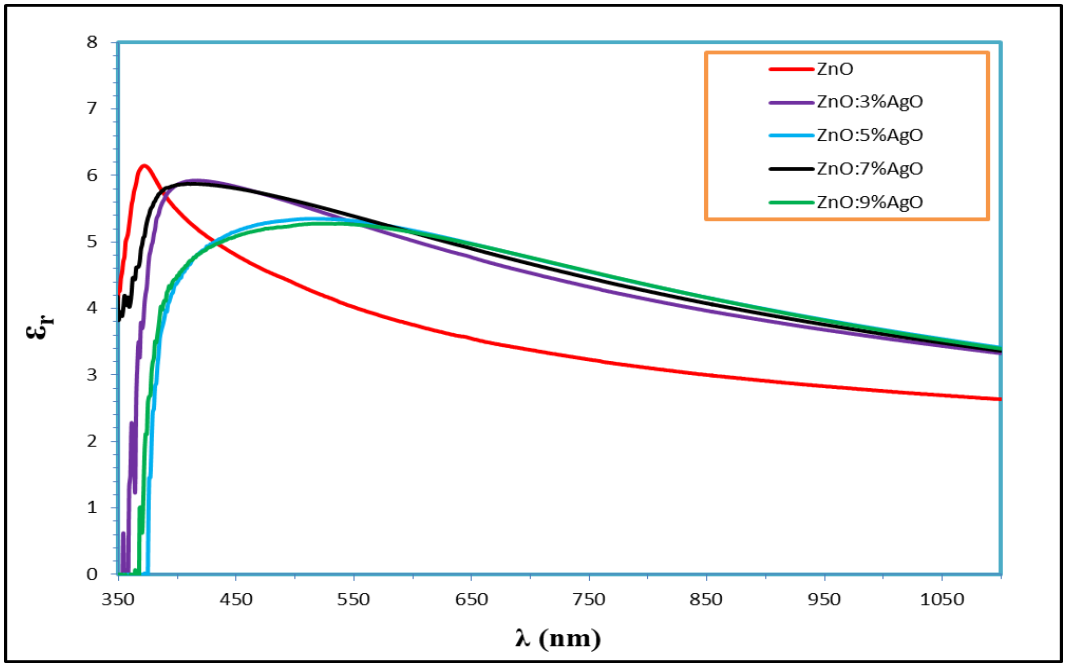

Figure 7-The plot diagram of ε_r versus wavelength for ZnO:AgO thin films prepared by PLD technique

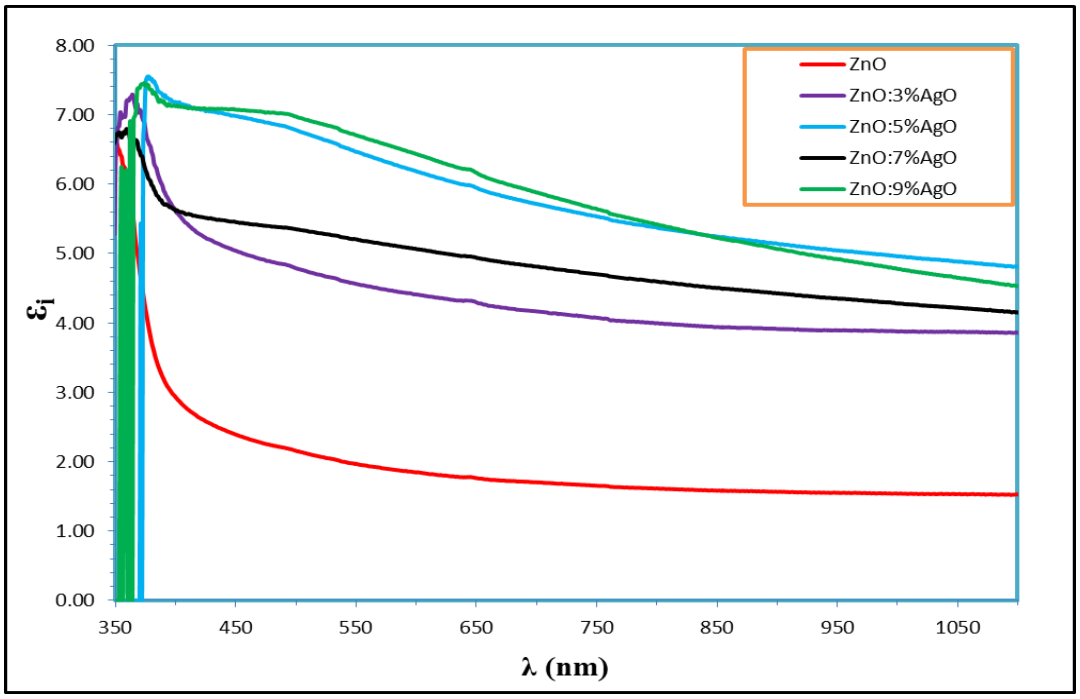

Figure 8- The plot diagram of ε_i versus wavelength for ZnO:AgO thin films prepared by PLD technique

Table 3-Transmittance , absorption coefficient , optical constants at λ=550nm,and optical energy gap of ZnO:AgO thin films prepared by PLD technique.

sample	T%	α (cm^{-1})	k	n	ε_r	ε_i	Eg (eV)
ZnO	76.12	109162	0.478	2.062	4.025	1.972	3.21
ZnO:3%AgO	59.12	210264	0.921	2.478	5.293	4.563	3.2
ZnO:5%AgO	49.40	282118	1.235	2.616	5.320	6.465	3.15
ZnO:7%AgO	55.68	234215	1.026	2.538	5.389	5.206	3.15
ZnO:9%AgO	48.24	291560	1.277	2.626	5.265	6.705	2.95

Conclusion:

Pure and AgO-doped ZnO thin films were successfully fabricated by pulsed laser deposition method. The XRD patterns showed wurtzite structure for all the prepared thin films samples and no impurity phase was noted. The maximum crystallite size obtained from XRD was 22.4 nm. The UV-Visible results revealed that absorption underwent a redshift with AgO into ZnO as compared to pure ZnO exhibiting strong quantum confinement effects. Optical band gap energy was found to decrease from 3.21 to 2.91 eV with AgO doping, resulting in the increment in their crystallite size as a result of Ag doping. It could be concluded that defects play an important role in manipulating properties of ZnO thin film

References

[1] T. Chitradevi, A. J. Lenus, and N. V. Jaya, "Structure, morphology and luminescence properties of sol-gel method synthesized pure and Ag-doped ZnO nanoparticles," *Mater. Res. Express*, vol. 7, no. 1, p. 15011, 2019.

[2] Ö. A. Yıldırım, H. E. Unalan, and C. Durucan, "Highly efficient room temperature synthesis of silver-doped zinc oxide (ZnO: Ag) nanoparticles: structural, optical, and photocatalytic properties," *J. Am. Ceram. Soc.*, vol. 96, no. 3, pp. 766–773, 2013.

[3] S. Sagadevan, K. Pal, Z. Z. Chowdhury, and M. E. Hoque, "Structural, dielectric and optical investigation of chemically synthesized Ag-doped ZnO nanoparticles composites," *J. Sol-Gel Sci.*

Technol., vol. 83, no. 2, pp. 394–404, 2017.
[4] M. Rezapour and N. Talebian, "Comparison of structural, optical properties and photocatalytic activity of ZnO with different morphologies: Effect of synthesis methods and reaction media," *Mater. Chem. Phys.*, vol. 129, no. 1–2, pp. 249–255, 2011.
[5] Ş. Ş. Türkyılmaz, N. Güy, and M. Özacar, "Photocatalytic efficiencies of Ni, Mn, Fe and Ag doped ZnO nanostructures synthesized by hydrothermal method: The synergistic/antagonistic effect between ZnO and metals," *J. Photochem. Photobiol. A: Chem.*, vol. 341, pp. 39–50, 2017.
[6] F. Xian, K. Miao, X. Bai, Y. Ji, F. Chen, and X. Li, "Characteraction of Ag-doped ZnO thin film synthesized by sol-gel method and its using in thin film solar cells," *Optik (Stuttg).*, vol. 124, no. 21, pp. 4876–4879, 2013, doi: 10.1016/j.ijleo.2013.02.034.
[7] S. Faÿ, U. Kroll, C. Bucher, E. Vallat-Sauvain, and A. Shah, "Low pressure chemical vapour deposition of ZnO layers for thin-film solar cells: temperature-induced morphological changes," *Sol. Energy Mater. Sol. Cells*, vol. 86, no. 3, pp. 385–397, 2005.
[8] S. Elmas and Ş. Korkmaz, "Deposition of Al doped ZnO thin films on the different substrates with radio frequency magnetron sputtering," *J. Non. Cryst. Solids*, vol. 359, no. 1, pp. 69–72, 2013.
[9] B.-Z. Dong, G.-J. Fang, J.-F. Wang, W.-J. Guan, and X.-Z. Zhao, "Effect of thickness on structural, electrical, and optical properties of ZnO: Al films deposited by pulsed laser deposition," *J. Appl. Phys.*, vol. 101, no. 3, p. 33713, 2007.
[10] S. Golshahi, S. M. Rozati, R. Martins, and E. Fortunato, "P-type ZnO thin film deposited by spray pyrolysis technique: The effect of solution concentration," *Thin Solid Films*, vol. 518, no. 4, pp. 1149–1152, 2009.
[11] H. Kato, M. Sano, K. Miyamoto, and T. Yao, "Growth and characterization of Ga-doped ZnO layers on a-plane sapphire substrates grown by molecular beam epitaxy," *J. Cryst. Growth*, vol. 237, pp. 538–543, 2002.
[12] K. Y. Cheong, N. Muti, and S. R. Ramanan, "Electrical and optical studies of ZnO: Ga thin films fabricated via the sol–gel technique," *Thin Solid Films*, vol. 410, no. 1–2, pp. 142–146, 2002.
[13] H.-M. Shabana, "Determination of film thickness and refractive index by interferometry," *Polym. Test.*, vol. 23, no. 6, pp. 695–702, 2004.
[14] J. Epp, "X-ray diffraction (XRD) techniques for materials characterization," in *Materials characterization using nondestructive evaluation (NDE) methods*, Elsevier, 2016, pp. 81–124.
[15] P. Bindu and S. Thomas, "Estimation of lattice strain in ZnO nanoparticles: X-ray peak profile analysis," *J. Theor. Appl. Phys.*, vol. 8, no. 4, pp. 123–134, 2014.
[16] J. Tauc and F. Abeles, "Optical Properties of Solids North-Holland." Amsterdam, 1970.
[17] M. Kemell, F. Dartigues, M. Ritala, and M. Leskelä, "Electrochemical preparation of In and Al doped ZnO thin films for CuInSe2 solar cells," *Thin Solid Films*, vol. 434, no. 1–2, pp. 20–23, 2003.
[18] T. ALWAN and M. JABBAR, "Structure and optical properties of CuAlS_2 thin films prepared via chemical bath deposition," *Turkish J. Phys.*, vol. 34, no. 2, pp. 107–116, 2011.
[19] A. F. Lotus, Y. C. Kang, J. I. Walker, R. D. Ramsier, and G. G. Chase, "Effect of aluminum oxide doping on the structural , electrical , and optical properties of zinc oxide (AOZO) nanofibers synthesized by electrospinning," vol. 166, pp. 61–66, 2010, doi: 10.1016/j.mseb.2009.10.001.
[20] W. Khan, Z. A. Khan, A. A. Saad, S. Shervani, A. Saleem, and A. H. Naqvi, "Synthesis and characterization of Al doped ZnO nanoparticles," in *International Journal of Modern Physics: Conference Series*, 2013, vol. 22, pp. 630–636.
[21] Z. Chen, S. Li, Y. Tian, S. Wu, and W. Zhang, "Sythesis of magnesium oxide doped ZnO nanostructures using electrochemical deposition," *Int. J. Electrochem. Sci*, vol. 7, pp. 10620–10626, 2012.
[22] D. Yao, J. Yang, Y. Xie, Y. Wang, Y. Wang, and H. Li, "Warm white-light phosphor based on a single-phase of Ag+/Eu3+/Zn2+ loading SOD zeolites with application to white LEDs," *J. Alloys Compd.*, vol. 823, p. 153778, 2020.
[23] I. Avramova, G. K. Mani, and T. M. Hammad, "Ag doped Zno."????
[24] C. Karunakaran, V. Rajeswari, and P. Gomathisankar, "Combustion synthesis of ZnO and Ag-doped ZnO and their bactericidal and photocatalytic activities," *Superlattices Microstruct.*, vol.

50, no. 3, pp. 234–241, 2011.

[25] M. Karyaoui, A. Mhamdi, H. Kaouach, A. Labidi, A. Boukhachem, K. Boubaker, M. Amlouk, R. Chtourou, "Some physical investigations on silver-doped ZnO sprayed thin films," *Mater. Sci. Semicond. Process.*, vol. 30, pp. 255–262, 2015.

[26] M. A. Subhan, A. M. M. Fahim, P. C. Saha, M. M. Rahman, K. Begum, and A. K. Azad, "Structural study, photoluminescence and photocatalytic properties of La2O3· Fe3O4· ZnO, AgO· NiO· ZnO and La2O3· AgO· ZnO nanocomposites," *Nano-Structures & Nano-Objects*, vol. 10, pp. 30–41, 2017.

[27] H. Sutanto, S. Wibowo, I. Nurhasanah, and E. Hidayanto, "Optical and microstructure of thin film of Ag-doped ZnO synthesized by sol-gel," in *AIP Conference Proceedings*, 2016, vol. 1755, no. 1, p. 150001.

[28] SYED MANSOOR ALI, W.A. FAROOQ , M.R. BAIG , M.A. SHAR , M. ATIF ,S.S. ALGHAMDI , M.S. ALGARAWI , NAEEM-UR-REHMAN , MUHAMMAD HAMMAD AZIZ "Structural and optical properties of pure and Ag doped ZnO thin films obtained by sol gel spin coating technique," *Mater. Sci.Poland*, vol. 33, no. 3, pp. 601–605, 2015.

[29] N. Serpone, D. Lawless, and R. Khairutdinov, "Size effects on the photophysical properties of colloidal anatase TiO2 particles: size quantization versus direct transitions in this indirect semiconductor?," *J. Phys. Chem.*, vol. 99, no. 45, pp. 16646–16654, 1995.